Indian Journal of Pure & Applied Physics
Vol. 52, February 2014, pp. 93-100

Synthesis and characterization of dodecanethiol-stabilized gold nanoparticles

Ankita Sharma[1], Bhanu P Singh[2]* & Arvind K Gathania[1]

[1]Department of Physics, National Institute of Technology, Hamirpur, Himachal Pradesh 177 005, India

[2]Department of Physics, Indian Institute of Technology, Bombay, Powai, Mumbai 400 076, India

*E-mail: akgathania@yahoo.com

Received 16 July 2013; revised 30 September 2013; accepted 18 December 2013

Dodecanethiol-stabilized gold nanoparticles of different sizes were synthesized using Bi-phasic reduction method by varying the concentration of stabilizer. These particles were characterized using transmission electron microscopy (TEM), Fourier transform infrared spectroscopy (FTIR) and ultraviolet-visible spectroscopy (UV-Vis). TEM images show the average particle size of different samples ranging from ~1.7 nm to 5.7 nm. FTIR study confirms the linkage of thiol group and their partial crystalline self assembly onto the surface of nano gold particles. From the UV-Vis spectra, it is noticed that absorption peak position is sensitive to the size of the particles. Theoretical fit for absorbance spectra was obtained using Mie theory and the deviation from experimental results demonstrates the large size and shape distribution. A linear relationship between logarithms of extinction coefficient and particle diameter is obtained, which explains the extinction coefficient dependence on the size of the particle.

Keywords: Nanoparticles, Fourier transform infrared spectroscopy, Transmission electron microscopy, Ultraviolet-visible spectroscopy

1 Introduction

Nanoparticles have attracted considerable scientific and technological interests worldwide by many researchers[1-6]. In particular, gold nanoparticles (AuNPs) have been studied and synthesized extensively because of their size and shape dependent properties and for a wide range of applications in the field of nanophotonics[7], optoelectronics[8] drug delivery[9], catalysis[10], surface enhanced Raman spectroscopy[11,12] (SERS). Different methods have been developed to synthesize the nano-range particles and it has been found that the different sized nanoparticles can be synthesized by varying the ratios among the reagents. The particles in the nano-range are highly unstable and they tend to agglomerate, in order to overcome this problem they are generally stabilized using different ligands like-amines[13], citrates[14], thiols[15] etc. Frens *et al*[16]. synthesized AuNPs with a broad size range from 10 to 150 nm by varying the citrate to gold ratio and Leff *et al*[17]. obtained AuNPs with size ranging from 1.5 to 20 nm by varying the thiol to gold ratio. So by manipulating the reaction conditions, one can obtain particles of desired size and shape.

In the present paper, the synthesis of dodecanethiol-stabilized gold nanoparticles with the average size ranging from 1.7 to 5.7 nm, by varying the stabilizer to gold ratios, has been presented. The particles were characterized by transmission electron microscopy (TEM), Fourier transform infrared spectroscopy (FTIR), and UV-visible spectroscopy (UV-Vis). Theoretical fit for the experimental data of absorbance spectra has also been obtained.

2 Theoretical Background

Gold nanoparticles (AuNPs) are known to show a very intense surface plasmon absorption band in the visible region (typically around 520 nm) of the electromagnetic spectrum. This is the reason for the colour of gold nanoparticles. The exact position of this band depends on the size and shape of particles and properties of the surrounding medium. Mie was the first to describe them quantitatively by solving Maxwell's equations with appropriate boundary conditions for spherical particles. The extinction coefficient can be calculated by using the equations derived by Mie. The absorption coefficient $[\sigma(\omega)]$ in the quasi-static approximation (where the electromagnetic phase is assumed to be constant throughout the particle which is much smaller than the wavelength of light) for a particle of radius R having $\varepsilon_1(\omega)$ and $\varepsilon_2(\omega)$ real and imaginary parts of dielectric constant surrounded by medium with dielectric constant ε_m at frequency (ω) and λ wavelength of light is given by:

$$\sigma(\omega)=\frac{24\pi^2\varepsilon_m^{3/2}R^3}{\lambda}\frac{\varepsilon_2(\omega)}{\left[\varepsilon_1(\omega)+2\varepsilon_m\right]^2+\varepsilon_2^2(\omega)} \quad \ldots (1)$$

The resonant frequency is determined by the condition[14] $\varepsilon_1(\omega) + 2\,\varepsilon_m = 0$. The real and imaginary parts of the dielectric constant of absorbing material, in terms of bound electrons (*b*) and free electron (*f*) contributions are given by:

$$\begin{aligned}\varepsilon_1(\omega)&=\varepsilon_{1b}+\varepsilon_{1f}\\ \varepsilon_2(\omega)&=\varepsilon_{2b}+\varepsilon_{2f}\end{aligned}, \quad \ldots (2)$$

which suggests that the complex dielectric function of gold has a contribution from bound as well as free electrons. The free electron contributions can be calculated at frequency (ω_o) of inelastic collisions of free electron within the metal as:

$$\begin{aligned}\varepsilon_{1f}&=1-\frac{\omega_p^2}{\omega^2+\omega_o^2}\\ \varepsilon_{2f}&=\frac{\omega_p^2\omega_o}{\omega(\omega^2+\omega_o^2)}\end{aligned} \quad \ldots (3)$$

For gold, value of ω_o is 0.12×10^{15}/s. ω_p is the plasma frequency of free electrons and is expressed in terms of free electron density (n_e), electron charge (e) and effective mass m_e as:

$$\omega_p^2=\frac{\pi n_e e^2}{m_e} \quad \ldots (4)$$

showing that plasma frequency depends only on free electron density. If we assume that all the valence electrons (Z_V) of each gold atom contribute to free electron gas, free electron density can be calculated using the relation:

$$n_e=\frac{N_A Z_V \rho}{A} \quad \ldots (5)$$

with A is the atomic weight (g/mol), N_A the Avogadro's number (6.02×10^{23} atoms/mol), ρ is the density (g/cm^3). For gold, it comes out to be 5.9×10^{22}/cm^3. The value of plasma frequency for gold is 1.3×10^{16} s^{-1}. In the nanoparticles of size below ~10 nm, the dielectric functions $\varepsilon_1(\omega)$ and $\varepsilon_2(\omega)$ exhibit size dependence behaviour. Mean free path effect is the strongest for these particles as compared to n_e, m_e *etc.* parameter dependence. The mean free path factor contributes in the increase of the surface scattering rate (ω_s) in comparison to the bulk scattering (ω_o). This contribution as a correction in the Mie theory by modifying the dielectric function for the particles in this range is expressed as:

$$\omega_s=\frac{Bv_f}{R}, \quad \ldots (6)$$

where v_f is Fermi velocity (1.4×10^8 cm/s for gold). R the radius of the nanoparticle and B is the proportionality factor which is of the order of unity for isotropic scattering. Therefore, size dependent dielectric function is obtained from Eq. (3) using ω_s in place[19] of ω_o. The bound electron contribution has been taken from the data given by Jhonson and Christy[20].

3 Materials and Methods

Materials used: Hydrogen tetrachloroaurate (III) hydrate ($HAuCl_4.3H_2O$), was obtained from Acros, Fishers Scientific. Dodecanethiol (DT), Tetra octyl ammonium bromide (TOAB), Sodium borohydride ($NaBH_4$), and ethanol were purchased from Merck-India. All the chemicals were used as received without any further purification. Deionized water used in preparation had a resistivity of 18.2 MΩ obtained from Lab Pure Andel BIO-AGE.

Dodecanethiol-stabilized gold nanoparticles have been synthesized using Bi-phasic reduction method[21]. $HAuCl_4$ was used as a gold source and TOAB as a phase-transfer agent. In this scheme, $AuCl_4^-$ ions are transferred from aqueous $NaBH_4$, in the presence of DT to the organic phase. AuNPs of different sizes were obtained by varying the gold to thiol ratio, in the following manner: 0.557 g (0.099 M) TOAB was mixed with 10 ml toluene and stirred for 10 min, then 0.18 g (0.0305 M) of $HAuCL_4.3H_2O$ was dissolved in deionized water with constant stirring for 10 min. These two solutions were then mixed together and stirred until the organic phase turned orange in colour and the aqueous phase became clear. The organic phase was separated using a separation funnel and DT (in varying concentrations; in order to have different gold to thiol ratios; eg. for 1:1 ratio, 0.458 M of DT in 3.13 ml toluene) was added and stirred for about 10 min. Further, this solution was reduced slowly with 0.19 g (0.0418 M) of $NaBH_4$ aqueous solution, which was added drop-wise, over the period of 30 min, to the solution. The final solution was stirred

for next 12 h. Again the organic phase was separated from the aqueous phase and ethanol was mixed in this phase with constant stirring until the precipitates fell out of the solution. It was then centrifuged at 3500 rpm for 15 min. Precipitates were redispersed in toluene and stored for further characterizations. In this manner, 7 samples were prepared by varying the gold/thiol ratio as 1:1-6:1 while keeping all other concentrations same. The reactions involved in the synthesis are:

Phase transfer of a gold salt:

$$HAuCl_4(aq)+BrN(C_8H_{17})_4(tol) \rightarrow$$
$$N(C_8H_{17})_4^+(AuCl_4)^-(tol)+HBr(aq)$$

Reduction of Au(III) to Au(0) and stabilization:

$$m(AuCl_4)^-(tol)+n(C_{12}H_{25}SH)(tol)+3me^- \rightarrow$$
$$4mCl^-(aq)+(Au_{m-n})(C_{12}H_{25}S\text{-}Au)_n(tol)$$

source of electrons is BH_4^-. The conditions of the reaction determine the ratio of gold to stabilizer (DT), i.e. the ratio m/n. (m:n = 1:1-6:1).

All the samples were characterized by Fourier transform infrared spectroscopy (PerkinElmer Spectrum 65 spectrometer), high resolution transmission electron Microscopy (Hitachi-7500), at room temperature. The samples were also characterized using Ultraviolet-Visible-NIR spectroscopy (Perkin-Elmer, LAMBDA 750).

4 Results and Discussion

To investigate the effect of gold to thiol ratio on the particle size, the samples were characterized using TEM. The samples were prepared as: a droplet of solution of AuNPs in toluene was evaporated onto the carbon-coated side of a mesh copper TEM grid. Figure 1 shows that the particles are in nano-range, nearly spherical in shape and reasonably uniform in size except for molar ratio 5:1. We also noticed shapes like triangles, squares and rectangles only at this ratio. TEM images also show the dependence of the particle size on the gold/thiol ratio. A quantitative relation is also possible between the shape and gold/thiol ratio through carrying the experiment at other concentrations. The particle size distribution was also measured by sampling about 200 particles for each sample and the histograms were obtained. The histograms were then fitted with log normal function and the distributions obtained were plotted along with histograms. The statistical analysis of the particles, for all samples, revealed that there is a size distribution of about 10-20% mean standard deviation (σ). The obtained particle size (D) range was 1.7 to 5.7 (D) nm. The detailed results (average particle size ($\langle D \rangle$), standard deviation (SD) and skewness) are given in the Table 1. From the TEM analysis, we have calculated the concentrations of NP solution for each sample[22]. Assuming spherical shape and uniform *fcc* structure, first the average number of gold atoms (N) within a NP, for each sample was calculated using the radius of NP (R_{NP}) and that of gold atom (R_{atom}) as:

$$N = \left(\frac{R_{NP}}{R_{atom}} \right)^3 . \quad \ldots (7)$$

Considering the reduction was complete and all the gold salt added was reduced to gold atoms, the concentration (C) of each sample was calculated. The number of atoms present in the initial concentration used (say 'x'M) were calculated as:

$$N_{atom} = x \times N_{A,} \quad \ldots (8)$$

where N_A is the Avogadro's number, hence number of nanoparticles formed in the colloidal solution were given by:

$$N_{NP} = \frac{N_{atom}}{N} \quad \ldots (9)$$

and the corresponding amount of NPs formed (N_{NP}), are:

$$C = \frac{N_{NP}}{N_A}. \quad \ldots (10)$$

The concentrations of different samples with different particle size are given in Table 1.

FTIR is used to detect the functional groups and study the vibrational motion of atoms or molecules. FTIR spectra were taken on NaCl disc prepared by drop-casting the AuNPs solution in toluene and also the pure DT as shown in Fig. 2. It was observed that most of the characteristic bands[23] of AuNPs resemble those of pure DT, which indicates that thiol is indeed a part of the composition. The samples exhibited two bands at 654 and 722 cm^{-1} for DT and 694 and 728 cm^{-1} for AuNPs, attributed to the C-S stretching bands (*Gauche* and *Trans*, respectively) of the thiol group. From the FTIR spectroscopy, it is possible to estimate

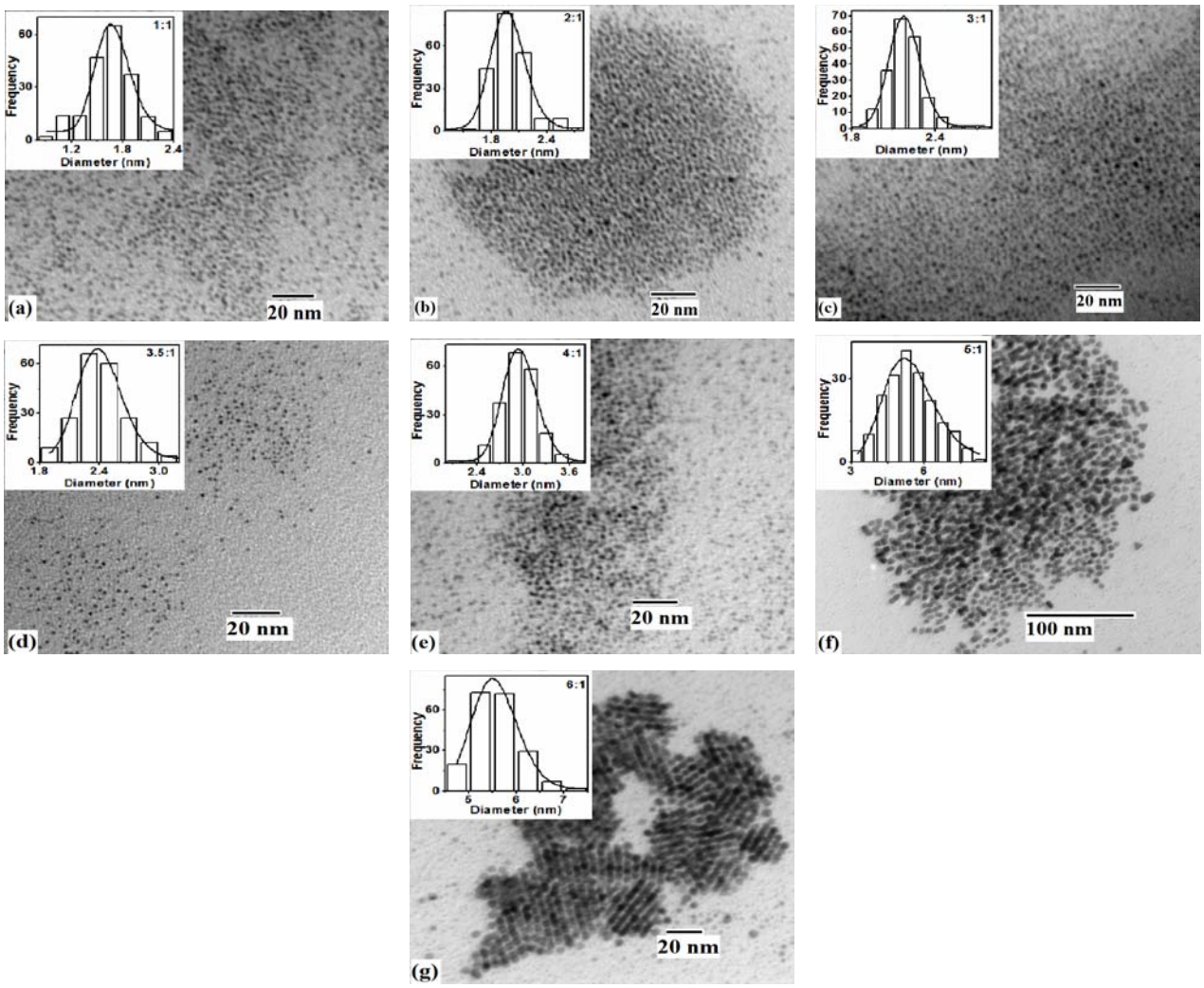

Fig. 1 — TEM images of AuNPs and their respective size distribution histograms. The fit to a log normal function is also shown plotted along the histograms

Table 1 — Parameters from the particle size distributions

Sr. No.	Au:S	*n*	<*D*> (nm)	SD	Skewness	*C* (moles/L)	ε_x (M^{-1} cm^{-1})
1	1:1	197	1.702	0.49	-0.038	1.6E-5	3.25E+4
2	2:1	204	2.008	0.49	+0.067	9.7E-6	5.59E+4
3	3:1	203	2.208	0.303	+0.052	7.28E-6	7.50E+4
4	3.5:1	207	2.48	0.49	+0.083	5.14E-6	1.09E+5
5	4:1	202	2.811	0.548	0.033	3.53E-6	1.61E+5
6	5:1	194	5.55	1.658	+0.07	4.58E-7	1.24E+6
7	6:1	203	5.72	0.935	+0.082	4.19E-7	1.43E+6

the defects at the gold/organic interface which are recognized through the relative absorbance of C-S stretching vibrations for *trans* (~720 cm^{-1}) and *gauche* (~650 cm^{-1}) defect[24]. It is observed from the spectra that the *gauche* defect absorbance decreases in comparison to the *trans* absorbance, which implies that the adsorbed layer has a defect free uniformity and crystallinity onto the gold surfaces.

Rougher Au surfaces imply more near-surface defects[25]. The lower frequency region, 1100-1500 cm^{-1}, corresponds to the C–H bending, wagging and C-C stretching vibration modes[24]. The 1638 and

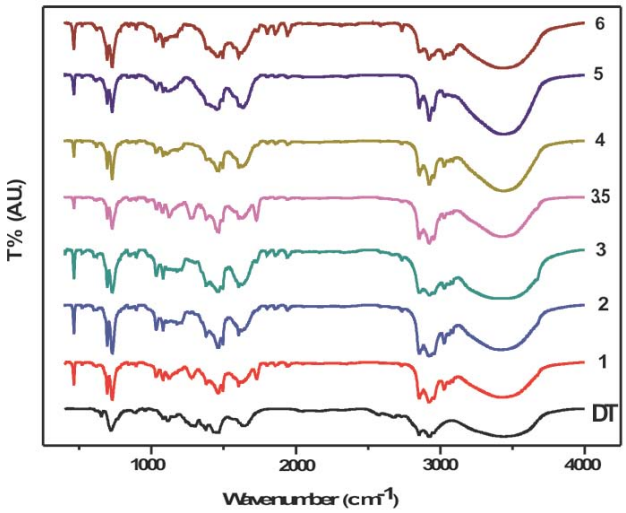

Fig. 2 — FTIR spectra of Pure DT and all the samples

1730 cm^{-1} bands represent the C=O stretching vibration frequency of carboxylic group. The absorbance of this band increases with the gold ratio. This may be attributed to the impurity present in the samples. Region from 1700 to 2000 cm^{-1} corresponds to the overtones of aromatic ring (toluene). Another region which is present in AuNPs is 3000-3100 cm^{-1}, corresponding to =C–H stretch in aromatics. S-H vibration band at 2576 cm^{-1} for pure DT is observed while it is almost absent for AuNPs. This suggests that as the thiol gets bound onto the surface of gold, the S-H bond of thiol breaks in order to form the S-Au bond[26].

The region 2800-3000 cm^{-1} is the C-H stretching region. The assembly of the long chain thiols onto a surface is, generally, predicted by the position of ν_{as} (CH) signal, which is found to be in the range 2925-2916 cm^{-1} depending on the chain conformation. The position of the CH_x band maxima indicates, in all cases, a lower level of *gauche*-defects with respect to the liquid as a result of interactions between the alkyl chains and suggests a partial crystalline self assembly of DT molecules onto the surface[27] of AuNPs. Bands corresponding to asymmetric and symmetric methylene stretching are observed at 2924 and 2854 cm^{-1}, respectively. The absorbance of methylene stretching decreases with increasing gold to thiol ratio. It may be attributed to the relative decrease of the volume fraction of capping agent (thiol) with the increase in core diameter. Bands for asymmetric and symmetric methyl stretching are also present[28] for AuNPs at 2956 and 2872 cm^{-1}, respectively.

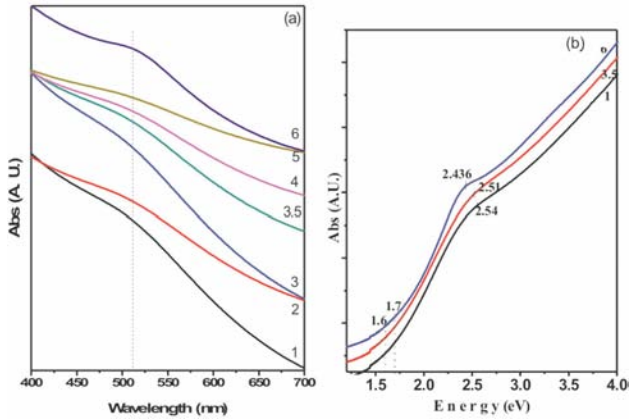

Fig. 3 — UV-Vis spectra of gold nanoparticles (a) of different gold to thiol ratio and (b) on a semi-lograthmic scale (Absorbance versus Energy) for 1:1, 3.5:1 and 6:1 gold to thiol ratio samples

TEM images provided a very precise microstructural morphology which helps in explaining the observed UV-Vis absorption behaviour of the samples, as shown in Fig. 3(a). UV-Vis spectra were acquired at wavelengths between 400 and 700 nm of samples in quartz cells having 1 cm path length. Toluene was used as the reference and the blank for baseline subtraction. In general, the UV-Vis absorption spectra of AuNPs are dominated in the visible range by the presence of surface plasmon resonance (SPR) bands.

In this case, as the particles become smaller, a higher proportion of surface gold atoms is bound to sulphur (because of the increased surface to volume ratio), which in turn leads to the localization of the charge at the Au-S bond implying a decrease in the mobility of the free electrons and in turn the intensity of absorption in the surface plasmon region. For the smallest NP system (1:1), the observed absorbance is very weak and this is consistent with the theory[29].

As the gold/thiol ratio increased to 6:1, there was a noticeable increase in the intensity of SPR band at the absorbance maxima. This quantitatively suggests an increase in the particle size with increasing ratio, which is consistent with the results observed from TEM images. It is also noticed that the absorption peak gets broadened at 5:1 molar ratio which may be due to different shapes at this ratio. A further observation from analysis of these plots concerned the relative positions of the absorbance maxima. As the SPR peaks in all cases were very broad and not sharp, it was very difficult (especially for very small particles) to assign a definite value of λ_{max}, however absorbance maxima were centered on approximately 510 nm. In order to observe the red shift of λ_{max},

spectra for 1:1, 3:1 and 6:1 were plotted in terms of energy, as shown in Fig. 3(b) and it was observed that the absorbance maxima shifts from 2.54 eV (488.2 nm) for 1:1 to 2.436 eV (509.03 nm) for 6:1 ratio, which suggested the red shift of absorbance maxima with increasing diameter of nanoparticles. This may be attributed to the high polarizability of the $5d^{10}$ gold cores.

Another feature observed from the spectra was an onset to strong absorption located near 1.7 eV that became increasingly distinct at nano-order dimensions. These show a clean break from the preonset behaviour occurring at the energy 1.6 eV. This can be ascertained by considering the elementary facts of electronic structure of close-packed gold[30]. This behaviour is due to the interband transition between completely filled $5d^{10}$ band to empty energy levels (lowest unoccupied molecular orbital, LUMO) of the sp conduction band. The interband transition occurring between completely filled d-band to partially filled conduction band is shown in Fig. 4(b). Even in bulk gold, this interband excitation takes place at the X-point of the first Brillouin zone (Fig. 4a), corresponding to ~1.7 eV energetically; since the Fermi surface deviates from the free-electron sphere near the X and L point because of the van Hove singularities in the density of states[31].

The plot between logarithmic derivatives of absorbance with respect to the energy (Fig. 5) for the smallest system (1.7 nm) shows a continuous curve with a gradual decrease beyond 2 eV, which reflects that there is a continuum pattern of energy levels in the conduction band. This behaviour validates the metallic nature of the nanoparticles and does not indicate metal to semiconductor transition despite of size smaller than 2 nm in our study. This absence of metallic to semiconductor transition may be attributed to large size distribution (polydispersity) of our samples.

The experimental results validated with a support of theoretical calculation of absorption spectra for particles having different diameter. Absorption coefficients for different sized particles were calculated using Eq. (1). We have taken the contribution from bound as well as free electrons. The free electron contribution was taken into consideration to account for the probable additional electron density provided by the thiol ligand at the interface between the gold surface and capping agent. Figure 6 shows the comparative spectra of experimental and theoretical results. All the curves were normalized to unity at 4.1 eV and offset from each other for a clear comparison. A poor resemblance may be attributed to the size and shape effects of the particles. All the curves were normalized to unity at 4 eV and offset from each other for a clear comparison. The small deviations seen in

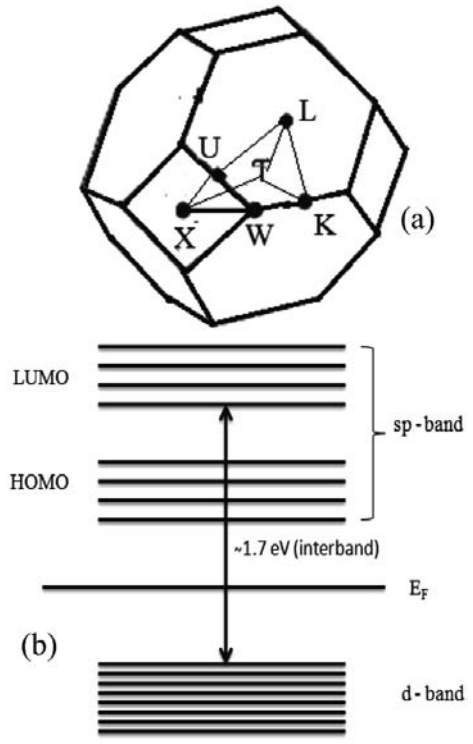

Fig. 4 — (a) Symmetry points in the first Brillouin zone of gold. (b) Band structure of gold close to the Fermi surface for the interband transition

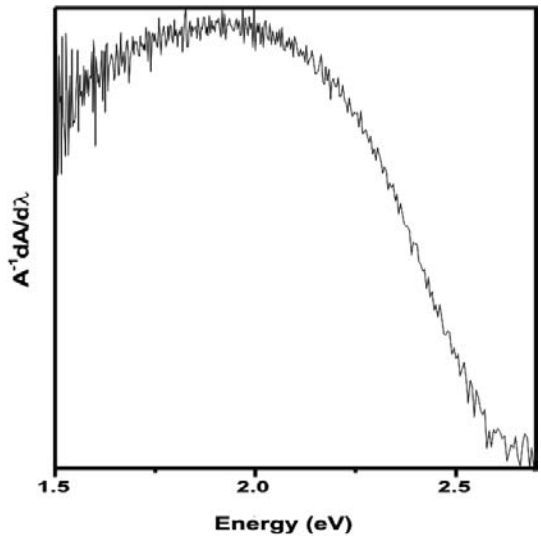

Fig. 5 — Logarithmic derivative (A^{-1} dA/dλ) of absorbance versus energy for the ~1.7 nm AuNPs

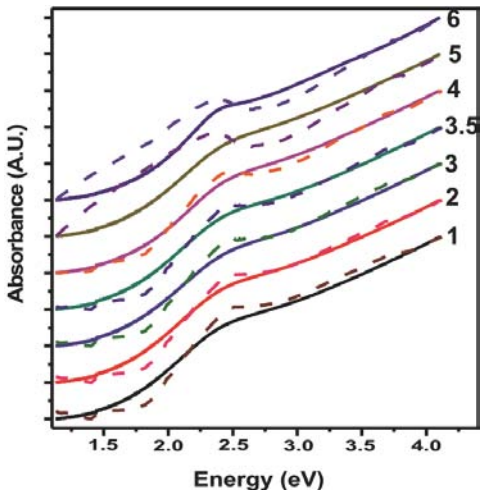

Fig. 6 — Experimental (solid) and theoretical (dash) absorption spectra of AuNPs prepared with different gold to thiol ratios

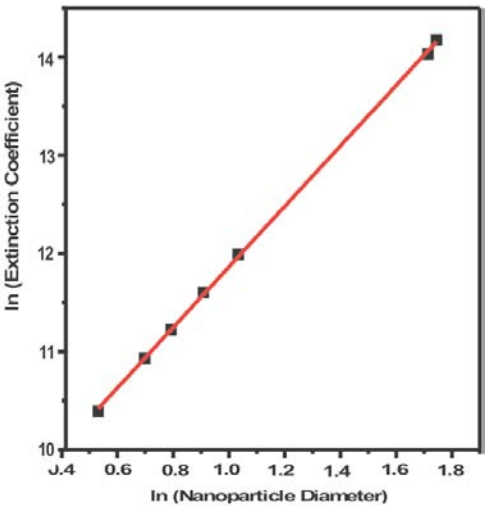

Fig. 7 — Experimental data and linear fitting curve of natural logarithm of extinction coefficient versus logarithm of average AuNP diameters

the absorption behaviour may be attributed to the size and shape effects of the particles.

The extinction coefficients (ε_x) of each NP sample was calculated from absorbance max (A_{max}), concentration of NP solution (C) and cuvette path length (l, which is 1 cm here) using the Lambert Beer Law as:

$$A_{max} = \varepsilon_x lC \quad \ldots (11)$$

All the values obtained are given in Table 1. From this Table 1, an important result is noticed that with the increase in the NP diameter, there is a dramatic increase in the extinction coefficients. From the double logarithm plot of extinction coefficient against the NP size in diameter (Fig. 7), a good linear relationship was found which can be expressed as:

$$\ln \varepsilon_x = k \ln D + a \quad \ldots (12)$$

where ε_x is in M^{-1} cm^{-1}, D is the NP diameter in nm. The straight line illustrates the dependence of molar extinction coefficient on the nanoparticles diameter in a linear fashion. This linear dependence is found to be in good agreement with Mie theory as demonstrated in Eq. (1). The values of k = 3.08355 and a = 8.7794 were found from the slope and intercept of the plot, respectively. These are found to be in good agreement with the reported experimental and theoretical values[32].

5 Conclusions

We prepared DT-stabilized AuNPs of different diameters by varying the concentration of DT and in turn the gold to thiol ratio. The samples have been studied using various characterization techniques viz. TEM, UV-Vis and FTIR. FTIR confirmed the absorption and partial crystalline self-assembly of DT molecules onto the Au surfaces and while TEM and UV-Vis could explain the effect of thiol ratio on the particle size and absorption spectra. TEM images show that particle diameter ranges from 1.7 nm to 5.7 nm for different samples by changing the Au/thiol ratio from 1 to 6. It is noticed that absorption peak is sensitive to the particles size and exhibits red-shift with increase in particle diameter. No quantum size effects were observed in the experimental results. Theoretical fit for absorbance spectra were obtained using Mie theory and the deviation from experimental results demonstrates the large size and shape distribution. A linear relationship obtained from the double logarithmic plot between extinction coefficients and nanoparticles diameter explains that the extinction coefficient depends on the particle diameter and increases linearly with the increase in particle diameter.

Acknowledgement

One of the authors (Ankita Sharma) is grateful to the National Institute of Technology, Hamirpur (HP), India for providing financial assistance.

References

1 Pitkethly M J, *Materials Today*, 7 (2010) 20.
2 Lee K-S & El-Sayed M A, *J Phys Chem,* 110 (2006) 19220.
3 Daniel M-C & Astruc D, *Chem Rev*, 104 (2004) 293.

4 Dhiman N, Singh B P & Gathania A K, *J Nanophotonics*, 6 (2012).
5 Behera D, Bag B & Sakthival R, *Indian J Pure & Appl Phys,* 49 (2011) 754.
6 Mercy A, Selvaraj R S, Boaz B M, Anandhi A & Kamagadurai R, *Indian J Pure & Appl Phys*, 51 (2013) 448.
7 Kamat P V, *J Phys Chem B*, 106 (2002) 7729.
8 Maier S A, Brongersma M L, Kik P G, Meltzer S, Requicha A A G & Atwater H A, *Adv Mater,* 13 (2001)1501.
9 Dreaden E C, Alkilany A M, Huang X, Murphy C J, El-Sayed M A, *Chem Soc Rev,* 41 (2012) 2740.
10 Zhou X, Xu W, Liu G, Panda D & Chen P, *J Am Chem Soc,* 132 (2010) 138.
11 R-Lorenzo L, A-Puebla R A, de Abajo F J G & L-Marzan L M, *J Phys Chem C,* 114 (2010) 7336.
12 Kumar G V P, *J Nanophoton*, 6 (2012) 064503-1-20.
13 Leff D V, Brandt L & Heath J R, *Langmuir,* 129 (1996) 4723.
14 Link S & El-Sayed M A, *J Phys Chem B,* 103 (1999) 4212.
15 Woehrle G H, Brown L O & Hutchison J E, *J Am Chem Soc,* 127, (2005) 2172.
16 Frens G, *Nature,* 241(1973) 201.
17 Leff D V, Ohara P C, Heath J R & Gelbart W M, *J Phys Chem*, 99 (1995) 7036.
18 Hovel H, Fritz S, Hilger A, Kreibig U & Vollmer M, *Phys Rev B*, 48 (1993) 18178.
19 Alvarez M M, Khoury J T, Schaff T G, Shafigullin M N, Vezmar I & Whetten R L, *J Phys Chem B,* 101 (1997) 3706.
20 Johnson P B & Christy R W, *Phys Rev* B, 6 (1972) 4370.
21 Brust M, Walker M, Bethell D, Schiffrin D J & Whyman R, *Chem Commun*, 7 (1994) 801.
22 Lewis D J, Day T M, MacPherson J V & Pikramenou Z, *Chem Commun,* (2006) 1433.
23 Kisailus D, Najarian M, Weaver J C & Morse D E, *Adv Mater,* 17 (2005) 1234.
24 Hostetler M J, Stokes J J & Murray R W, *Langmuir,* 12 (1996) 3604.
25 Hostetler M J, Wingate J E, Zhong C-J, Harris J E, Vachet R W, Clark M R, Londono J D, Green S J, Stokes J J, Wignall G D, Glish G L, Porter M D, Evans N D & Murray R W, *Langmuir*, 149 (1998) 17.
26 Chen S & Kimura K, *Langmuir*, 15 (1999) 1075.
27 Dablemont C, Lang P, Mangeney C, Piquemal J-Y, Petkov V, Herbst F & Viau G, *Langmuir,* 24 (2008) 5832.
28 Yee C K, Jordan R, Ulman A, White H, King A, Rafailovich M & Sokolov J, *Langmuir,* 15 (1999) 3486.
29 W Haiss, Thanh N T K, Aveyard J & Fering D G, *Anal Chem*, 79 (2007) 4215.
30 Rance G A, Marsh D H & Khlobystov A N, *Chem Phys Lett,* 460 (2008) 230.
31 Beversluis M R, Bouhelier A & Novotny L, *Phys Rev B*, 68 (2003) 115433(1-10).
32 Liu X, Atwater M, Wang J & Huo Q, *Colloids and Surfaces B: Biointerfaces,* 58 (2007) 3.